FULL PAPER

Dalton
www.rsc.org/dalton

Preparation and characterization of rhodium(III), iridium(III) and ruthenium(II) bearing 1,3- or 1,4-dithianes†

Yasuhiro Yamamoto,*‡ Shinobu Sakamoto, Yuka Ohki, Akihiro Usuzawa, Masanori Fujita and Tomoyuki Mochida

Department of Chemistry, Faculty of Science, Toho University, Miyama 2-2-1, Funabashi, Chiba 274-8510, Japan

Received 9th June 2003, Accepted 25th July 2003
First published as an Advance Article on the web 6th August 2003

Reactions of $[Cp^*MCl_2]_2$ (**1a**: M = Rh, **1b**: M = Ir) or $[(arene)RuCl_2]_2$ (**1c**: arene = *p*-cymene; **1d**: arene = C_6Me_6) with 1,3-dithiane (1,3-$S_2C_4H_8$) gave $[\{LMCl_2\}_2(1,3\text{-}S_2C_4H_8)]$ **2** and $[(LMCl_2)(1,3\text{-}S_2C_4H_8)]$ **3** (L = Cp*Rh, Cp*Ir, or (*p*-cymene)Ru, (C_6Me_6)Ru), depending on molar ratios between **1** and 1,3-dithiane. The reaction in the presence of KPF_6 afforded the corresponding ionic complexes $[LMCl(1,3\text{-}S_2C_4H_8)_2](PF_6)$ **4**. Complex **3a** was treated with **1b**, affording the heterobinuclear complex $[Cp^*RhCl_2(1,3\text{-}S_2C_4H_8)IrCl_2Cp^*]$ **2ab**. Complex **2ab** was obtained by a similar reaction of **3b** with **1a**, whereas reactions of **1c** with **3a** or **3b** gave homonuclear complexes **2c** and **2a** (or **2b**). Ionic complexes **4** were treated with **1**, generating homo- or hetero-trinuclear complexes $[\{LMCl(1,3\text{-}S_2C_4H_8)_2\}(L'MCl_2)_2](PF_6)$ **5** (L = Cp*Ir, L′M = Cp*Rh, Cp*Ir, or (*p*-cymene)Ru: L = Cp*Rh, L′M = (*p*-cymene)Ru). Reactions of **1** with 1,4-dithiane (1,4-$S_2C_4H_8$) were carried out in a 1 : 1 molar ratio, generating binuclear complexes $[(Cp^*MCl_2)_2(1,4\text{-}S_2C_4H_8)]$ (**6a**: M = Rh; **6b**: M = Ir) or $[\{(arene)RuCl_2\}_2(1,4\text{-}S_2C_4H_8)]$ (arene = *p*-cymene (**6c**), C_6Me_6 (**6d**)). Reaction of **1a** with an excess of 1,4-dithiane afforded a neutral mononuclear complex $[Cp^*RhCl_2(1,4\text{-}S_2C_4H_8)]$ **7a**, whereas the reactions of **1b** or **1c** generated the corresponding ionic complexes $[Cp^*IrCl(1,4\text{-}S_2C_4H_8)](Cl)$ **8b** and $[(p\text{-cymene})RuCl(1,4\text{-}S_2C_4H_8)](Cl)$ **8c**. Treatment in the presence of KPF_6 gave ionic complexes $[LM(1,4\text{-}S_2C_4H_8)](PF_6)$ (L = Cp*Rh (**9a**), Cp*Ir (**9b**), (*p*-cymene)Ru (**9c**)) Structures of **2a**, **2ab**, **3a**, **3c**, **4a**, **8b** and **9c** were confirmed by X-ray analyses.

Introduction

Metal-containing supramolecules and coordination polymers have attracted interest in recent years because there are many promising metal fragments available for the construction of novel supramolecular materials.[1] In these compounds square-planar complexes have been generally used as building blocks which occupy vertices.[2] We were interested in supramolecular complexes based on quasi-octahedral geometries bearing arene, cyclopentadienyl or pentamethylcyclopentadienyl groups, and their derivatives, since a new type of supramolecular series would be developed by introduction of these organic moieties. Octahedral building blocks can be assembled to form cubic, ladder-shaped or step-shaped structures. Recently we have reported stepwise assembly of the tetranuclear rhodium and iridium supramolecules bearing pentamethylcyclopentadienyl and binary ligands.[3]

Chemistry on thioether macrocyclic metal complexes has been investigated in various groups. In these complexes a metal atom sits generally in the macrocyclic thioether cores, which function as multidentate ligands.[4] Six-membered cyclic thioethers such as 1,3-dithiane, 1,4-dithiane and 1,3,5-trithiane form a variety of complexes with soft, borderline and hard metals.[5] Spectroscopic studies for these complexes have been developed; various fluxional phenomena have been studied by dynamic NMR spectroscopy. These molecular motions included six-membered ring reversal, pyramidal ligand-atom inversion, and platinum–methyl scrambling.[6] The dithiane and trithiane have potential as the building ligands in the construction of supramolecules and dendrimers containing metal atoms. We were interested in the preparation of bi-, tri- and polynuclear metal compounds by utilizing dithiane and trithiane as core centers in addition to spectroscopic interests.

We here report the preparation of dithiane complexes of ruthenium(II), rhodium(III) and iridium(III) containing arene or pentamethylcyclopentadienyl groups as metallic building blocks.

Experimental

All reactions were carried out under a nitrogen atmosphere. Dichloromethane was distilled over CaH_2 and diethyl ether was distilled over $LiAlH_4$. $[Cp^*MCl_2]_2$ (M = Rh,[7] Ir[8]) and $[(arene)RuCl_2]_2$[9] were prepared according to the literature. The infrared and electronic absorption spectra were measured on FT/IR-5300 and U-best 30 instruments, respectively. The ^1H NMR spectra were measured on a JEOL EPC400 instrument at 400 MHz, and $^{31}P\{^1H\}$ NMR spectra were measured at 161 MHz using $P(OMe)_3$ as an external reference. Dithianes are commercially available.

Preparation of dinuclear complexes

$[(Cp^*RhCl_2)_2(\mu\text{-}1,3\text{-dithiane})]$ 2a. A mixture of **1a** (52.5 mg, 0.085 mmol) and 1,3-dithiane (11.8 mg, 0.098 mmol) in CH_2Cl_2 (10 mL) was stirred at room temperature for 24 h. After the solvent was removed, the residue was washed with diethyl ether and recrystallized from CH_2Cl_2–diethyl ether to give reddish brown crystals of **2a** (54.6 mg, 87.1%). UV-vis (CH_2Cl_2): λ_{max} 418, 245 nm ^1H NMR ($CDCl_3$): δ $1.60,^A$ 1.67^B (s, Cp*, 30H), 2.21^{A+B} (m, H, 4H), 2.99^{A+B} (br, H, 2H), 4.14^{A+B} (br, H). A relative population is *ca.* 1 : 1.1. Anal. Calc. for $C_{24}H_{38}Cl_4Rh_2S_2\cdot 1/2CH_2Cl_2$: C, 37.69; H, 5.03. Found: C, 37.71; H, 5.09%.

$[(Cp^*RhCl_2)(\mu\text{-}1,3\text{-dithiane})(Cp^*IrCl_2)]$ 2ab. According to the above-mentioned procedure, reddish orange complex **2ab** (58.5 mg, 65.8%) was prepared from **3a** (50.0 mg, 0.116 mmol) and **1b** (56.3 mg, 0.071 mmol). UV-vis (CH_2Cl_2): λ_{max} 414, 340

† Electronic supplementary information (ESI) available: Crystal data and ORTEP figures for **2b**, **2ab** and **3c** and further experimental details. See http://www.rsc.org/suppdata/dt/b3/b306496d/

‡ Present address: The Institute of Scientific and Industrial Research, Osaka University, e-mail: yamamo24@sanken.osaka-u.ac.jp (or e-mail: yamamoto@chem.sci.toho-u.ac.jp).

DOI: 10.1039/b306496d

232 nm. ^{1}H NMR ($CDCl_3$): δ 1.67 (s, Cp*, 30H), 2.31 (br, CH_2, 3H), *ca.* 3.0 (complex, CH_2, 4H), *ca.* 3.2 (complex, CH_2, 2H), 5.28 (s, CH_2Cl_2). Anal. Calc. for $C_{24}H_{38}Cl_4IrRhS_2 \cdot 2CH_2Cl_2$: C, 30.87; H, 4.23. Found: C, 31.31; H, 4.24%.

[(Cp*RhCl$_2$)(1,3-dithiane)] 3a. A mixture of **1a** (302 mg, 0.488 mmol) and 1,3-dithiane (644 mg, 3.35 mmol) in CH_2Cl_2.10 mL. was stirred at room temperature for 24 h. After the solution was removed, the residue was washed with diethyl ether and recrystallized from CH_2Cl_2–diethyl ether, giving reddish brown crystals of **3a** (395 mg, 98%). UV-vis (CH_2Cl_2): λ_{max} 415, 244 nm. ^{1}H NMR ($CDCl_3$): δ 1.62 (s, Cp*, 30H), 2.19 (qnt, CH_2, 2H), 2.94 (br, CH_2, H), 2.94 (br, CH_2, H), 4.05 (b, CH_2, H). Anal. Calc. for $C_{14}H_{23}Cl_2RhS_2$: C, 39.17; H, 5.40. Found: C, 39.04; H, 5.40%.

[Cp*RhCl(1,3-dithiane)$_2$](PF$_6$) 4a. A mixture of **1a** (146.0 mg, 1.2 mmol), 1,3-dithiane (64.5 mg, 0.10 mmol) and KPF_6 (67.5 mg, 0.30 mmol) was stirred in acetone (15 mL) at room temperature. After 24 h, the solvent was removed, and the residue was washed with diethyl ether and extracted with CH_2Cl_2. The solution was concentrated to *ca.* 2 mL and diethyl ether was added, affording orange crystals of **4a** (95.6 mg, 80.0%). IR (Nujol): 839 cm^{-1}. UV-vis (CH_2Cl_2): λ_{max} 401, 325 nm. ^{1}H NMR ($CDCl_3$): δ 1.86 (s, Cp*, 15H), 3.66 (s, CH_2, 4H), 2.3–4.55 (m, CH_2, 12H), 5.12 (s, CH_2Cl_2). Anal. Calc. for $C_{18}H_{31}ClF_6PRhS_4 \cdot 1/2CH_2Cl_2$: C, 31.27; H, 4.61. Found: C, 31.67; H, 4.60%.

[{Cp*IrCl(1,3-dithiane)$_2$}(Cp*RhCl$_2$)$_2$](PF$_6$) 5ba. A mixture of **4b** (44.0 mg, 0.059 mmol) and **1a** (36.5 mg, 0.059 mmol) was stirred in CH_2Cl_2 (10 mL) at room temperature. After 6 h, the solvent was reduced to *ca.* 3 mL under the reduced pressure. The residue was washed with diethyl ether and recrystallization from CH_2Cl_2–hexane gave orange crystals of **5ba** (65.2 mg, 81.2%). IR (Nujol): 841 cm^{-1}. UV-vis (CH_2Cl_2): λ_{max} 408, ~340, 252 nm. ^{1}H NMR (CD_3COCD_3): δ 1.10 (t, J_{HH} = 7.2 Hz, CH_3), 1.66 (s, Cp*, 15H), 1.74 (s, Cp*, 15H), ~1.86, 2.20 (br, CH_2), 2.41 (br, CH_2), 3.39 (q, J_{HH} = 7.2 Hz, CH_2O, 4H). Anal. Calc. for $C_{38}H_{61}Cl_5F_6IrPRh_2S_4 \cdot 0.5Et_2O$: C, 34.60; H, 4.77. Found: C, 34.23; H, 4.74%.

[{Cp*IrCl(1,3-dithiane)$_2$}{(*p*-cymene)RuCl$_2$}$_2$](PF$_6$) 5bc. Orange complex, **5bc** (38.5 mg, 66.3%) was obtained from the reaction of **4b** (36.8 mg, 0.049 mmol) with **1c** (30.1 mg, 0.049 mmol) similarly to the preparation of **5ba**. IR (Nujol): 841 cm^{-1}. UV-vis CH_2Cl_2): λ_{max} *ca.* 420, 343 nm. ^{1}H NMR (CD_3COCD_3): δ 1.29 (d, J_{HH} = 7.0 Hz, CH(C*H*$_3$), 12H), 1.66 (s, Cp*, 30H), 2.22 (s, *p*-Me, 6H), 2.97 (septet, J = 7.0 Hz, CH, 2H), 2.7–3.2 (br, CH_2, 16H), 5.46, 5.63 (AB system, J_{HH} = 6.0 Hz, 8H), 5.28 (s, CH_2Cl_2). Anal. Calc. for $C_{38}H_{59}Cl_5F_6IrPRu_2S_4 \cdot 0.5CH_2Cl_2$: C, 32.95; H, 4.38. Found: C, 33.07; H, 4.32%.

[{Cp*RhCl(1,3-dithiane)$_2$}{(*p*-cymene)RuCl$_2$}$_2$](PF$_6$) 5ac. Similarly to the preparation of **5ba**, orange complex **5ac** (50.9 mg, 81.2%) was prepared from **4a** (32.5 mg, 0.049 mmol) and **1c** (30.3 mg, 0.0495 mmol). IR (Nujol): 839 cm^{-1}. UV-vis CH_2Cl_2): λ_{max} 413, 349, 243 nm. ^{1}H NMR ($CDCl_3$): δ 1.08 (t, J_{HH} = 7.2 Hz, *C*H$_3$CH$_2$O), 1.29 (d, J_{HH} = 7.0 Hz, CH(C*H*$_3$), 12H), 1.65 (s, Cp*, 15H), 2.22 (s, *p*-CH_3, 6H), 2.6–4.2 (br, CH_2, 16H), 2.97 (septet, J_{HH} = 7.0 Hz, 2H), 3.39 (q, J_{HH} = 7.2 Hz, CH_2O, 4H), 5.55, 5.59 (AB type, J_{HH} = 6.0 Hz, *p*-cymene, 8H). Anal. Calc. for $C_{38}H_{59}Cl_5F_6PRhRu_2S_4 \cdot 0.5Et_2O$: C, 36.72; H, 4.93. Found: C, 36.86; H, 4.87%.

[(Cp*RhCl$_2$)$_2$(1,4-dithiane)] 6a. Similarly to the preparation of **3a**, **6a** (169.8 mg, 47.3%) was obtained from the reaction of **1a** (300.8 mg, 0.487 mmol) with 1,4-dithiane (64.5 mg, 0.536 mmol). UV-vis (CH_2Cl_2): λ_{max} 420 nm. ^{1}H NMR ($CDCl_3$): δ 1.60^A, 1.66^B (s, Cp*, 15H), ~3.2, 4.8 (br, SCH_2, 8H). Intensity ratio: A : B = 1.15 : 1.0. Anal. Calc. for $C_{24}H_{38}Cl_4Rh_2S_2$: C, 39.04; H, 5.19. Found: C, 38.76; H, 5.05%.

[Cp*RhCl$_2$(1,4-dithiane)] 7a. Orange complex **7a** (98.4 mg, 70.8%) was obtained from the reaction of **1a** (100.0 mg, 0.16 mmol) with 1,4-dithiane (195.0 mg, 1.62 mmol), and recrystallization from CH_2Cl_2–hexane. FAB mass: *m*/*z* 393 ([M$^+$]) (M = cationic part). UV-vis (CH_2Cl_2): λ_{max} 418, 245 nm. ^{1}H NMR ($CDCl_3$): δ 1.65 (s, Cp*, 6H), 2.82 (s, SCH_2, 4H), 3.31 (s, CH_2, 4H). Anal. Calc. for $C_{14}H_{23}Cl_2RhS_2 \cdot 1.25CH_2Cl_2$: C, 36.57; H, 5.07. Found: C, 36.57; H, 4.96%.

[Cp*IrCl(μ-1,4-dithiane)](Cl) 8b. A mixture of **1b** (100 mg, 0.126 mmol) and 1,4-dithiane (152 mg, 1.26 mmol) in CH_2Cl_2.10mL. was stirred at room temperature for 24 h. After the solvent was removed, the residue was washed with diethyl ether and recrystallized from CH_2Cl_2–hexane, giving a yellow powder (71.8 mg, 54.8%) of **8b**. FAB mass: *m*/*z* 483 ([M$^+$]) (M = cationic part). UV-vis (CH_2Cl_2): λ_{max} 333sh, 325 nm. ^{1}H NMR ($CDCl_3$): δ 1.94 (s, Cp*, 15H), 3.06 (d, J_{HH} = 9.0 Hz, CHCH, 2H), 3.24 (d, J_{HH} = 9.0 Hz, CHCH, 2H), 3.49 (d, J_{HH} = 8.0 Hz, CHCH, 2H), 3.97 (d, J_{HH} = 8.0 Hz, CHCH, 2H). Anal. Calc. for $C_{14}H_{23}Cl_2IrS_2$: C, 32.42; H, 4.47. Found: C, 32.19; H, 4.42%.

[(*p*-cymene)RuCl(1,4-dithiane)](PF$_6$) 9c. A mixture of **1c** (112 mg, 0.183 mmol), 1,4-dithiane (231 mg, 1.92 mmol) and KPF_6 (101 mg, 0.55 mmol) in CH_2Cl_2 (10 mL) and acetone (10 mL) was stirred for 10 h at room temperature. The solvent was removed under reduced pressure. The residue was washed with hexane in order to remove an excess of 1,4-dithiane, and extracted with CH_2Cl_2. The solution was concentrated to *ca.* 3 mL and ether was added, giving brown crystals (70.0 mg, 71.4%) of **9c**. FAB mass: *m*/*z* 391 ([M]$^+$). IR (Nujol): 842 cm^{-1}. UV-vis (CH_2Cl_2): λ_{max} 401, 325 nm. ^{1}H NMR ($CDCl_3$): δ 1.42 (d, J_{HH} = 6.8 Hz, CH(C*H*$_3$), 6H), 2.49 (s, *p*-Me, 3H), 2.98 (septet, J_{HH} = 6.8 Hz, CH, 1H), 2.80, 3.23 (AB system, J_{HH} = 8.0 Hz, S–CH_2, 8H) 5.61, 5.84 (AB system, J_{HH} = 5.0 Hz, *p*-cymene, 4H). Anal. Calc. for $C_{14}H_{22}ClF_6PRuS_2$: C, 31.37; H, 4.14. Found: C, 31.37; H, 4.14%.

Crystal data collection

All complexes were recrystallized from CH_2Cl_2–diethyl ether or acetone–diethyl ether. Cell constants were determined from 20 reflections on a Rigaku four-circle automated diffractometer AFC5S. The crystal parameters along with data collections are summarized in Table 1. Intensities were measured by the 2θ–ω scan method using Mo-Kα radiation (λ = 0.71069). Throughout the data collection the intensities of three standard reflections were measured every 200 reflections as a check of the stability of the crystals and no decay was observed except for the crystal of **2ab** which showed 85% decay. Intensities were corrected for Lorenz and polarization effects. The absorption correction was made with the ψ-scan methods. Atomic scattering factors were taken from the usual tabulation of Cromer and Waber.[10] Anomalous dispersion effects were included in F_{calc};[11] the values of $\Delta f'$ and $\Delta f''$ were those Creagh and McAuley.[12] All calculations were performed using the teXsan crystallographic software package.[13]

Determination of the structures

All complexes except **2ab** solved by direct methods (SIR92) were solved by Patterson methods (DIRDIF94 PATTY). All non-hydrogen atoms for **3a**, **3b**, **8b** and **9c** and the non-hydrogen atoms except a solvated molecule for **2a**, **2ab** and **4a** were refined anisotropically using full-matrix least-squares based on

Table 1 Crystal data for $[(Cp^*RhCl_2)_2(1,3\text{-}C_4H_8S_2)]\cdot 2CH_2Cl_2$ **2a**, $[Cp^*RhCl_2(1,3\text{-}S_2C_4H_8)]$ **3a**, $[Cp^*RhCl(1,3\text{-}S_2C_4H_8)_2](PF_6)CH_2Cl_2$ **4a**, $[\{Cp^*Ir(\mu\text{-}1,4\text{-}S_2C_4H_8)\}Cl](Cl)$ **8b** and $[(p\text{-cymene})Ru(\mu\text{-}1,4\text{-}S_2C_4H_8)](PF_6)$ **9c**

Complex	**2a**	**3a**	**4a**	**8b**	**9c**
Formula	$C_{26}H_{42}Cl_8Rh_2S_2$	$C_{28}H_{46}Cl_4Rh_2S_4$	$C_{19}H_{33}Cl_3PF_6RhS_4$	$C_{14}H_{23}Cl_2IrS_2$	$C_{14}H_{22}ClF_6PRuS_2$
M_w	908.17	858.53	743.94	518.58	535.93
Crystal system	Monoclinic	Monoclinic	Monoclinic	Monoclinic	Monoclinic
Space group	$P2_1$ (no. 4)	$P2_1$ (no. 4)	$P2_1/n$ (no. 14)	$P2_1/n$ (no. 14)	$P2_1/n$ (no. 14)
a/Å	14.068(3)	8.796(3)	12.79(2)	13.637(3)	8.894(6)
b/Å	9.243(2)	15.317(3)	12.114(8)	9.363(6)	20.590(9)
c/Å	16.487(2)	13.054(4)	19.49(1)	14.055(4)	10.918(7)
β/°	115.25	98.76(3)	89.59(8)	109.00(2)	96.86(5)
V/Å^3	1821.4(6)	1738.2(9)	3020(4)	1696(1)	1984(1)
Z	2	2	4	4	4
D_c/g cm^{-3}	1.656	1.640	1.636	2.030	1.793
μ(Mo-Kα)/cm^{-1}	16.22	15.13	12.05	84.36	12.65
Scan rate/° min^{-1}	8.0	8.0	16	16.0	8
No. of relections	3419	3191	5325	2975	3940
No. observed	3419	2953 ($I > 2.0\sigma(I)$)	2821 ($I > 3.0\sigma(I)$)	2152 ($I > 3.0\sigma(I)$)	3490
No. variables	314	344	287	172	226
R; R_w [a,b]	0.063; 0.111 [b]	0.033; 0.099	0.141;0.223	0.033; 0.043 [a]	0.109; 0.129 [b]
$R1$ (reflections)	0.039 (2973)	0.033 (2953)	0.136 (2568)	0.033 (2152)	0.072 (2507)
GOF [c]	1.43	1.148	2.02	1.11	1.86

[a] $R = \Sigma||F_o| - ||F_c||/\Sigma|F_o|$ and $R_w = [\Sigma w(|F_o| - |F_c|)^2/w|F_o|^2]^{1/2}$ ($w = 1/\sigma^2(F_o)$). [b] $R = \Sigma(F_o^2 - F_c^2)/\Sigma F_o^2$ and $R_w = [\Sigma w(F_o^2 - F_c^2)^2/\Sigma w(F_o^2)^2]^{1/2}$ ($w = 1/\sigma^2(F_o)$); $R1 = \Sigma||F_o| - |F_c||/\Sigma|F_o|$ for $I > 2.0\sigma(I)$. [c] GOF $= [\Sigma w(|F_o| - |F_c|)^2/(N_o - N_p)]^{1/2}$.

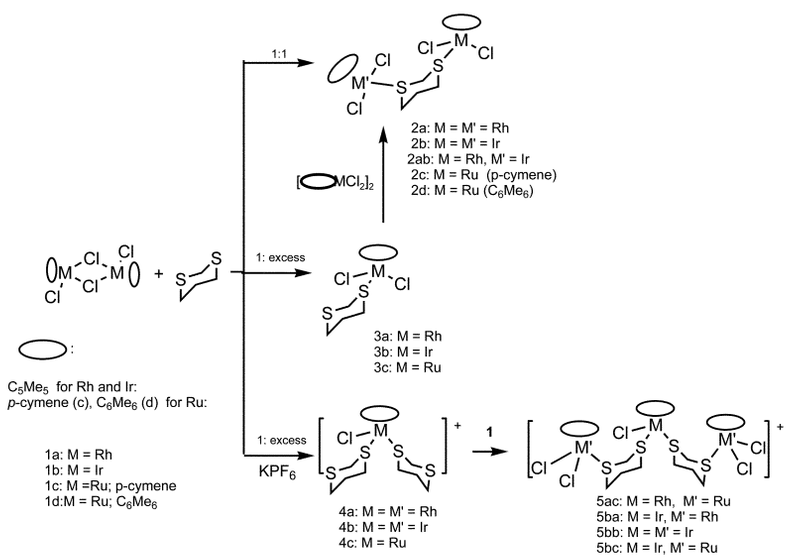

Scheme 1 Reactions of 1,3-dithiane; the PF_6 anion is removed for clarity.

F^2 (**2a** and **9c**) or F (**3a**, **2b**, **3c**, **4a** and **8b**). The non-hydrogen atoms of 25 atoms for **2b** and 16 atoms for **3c** were refined anisotropically. All hydrogen atoms were calculated at the ideal positions with the C–H distance of 0.95 Å.

CCDC reference numbers 211813–211816 and 211818–211821.

See http://www.rsc.org/suppdata/dt/b3/b306496d/ for crystallographic data in CIF or other electronic format.

Results and discussion

Homonuclear complexes

When 1,3-dithiane was treated with **1** in a 1 : 1 molar ratio at room temperature, complexes with an empirical formula of $[(Cp^*MCl_2)_2(C_4H_8S_2)]$ (**2a**: M = Rh; **2b**: M = Ir) or $[\{(arene)RuCl\}_2(S_2C_4H_8)]$ (**2c**: arene = *p*-cymene; **2d**: arene = C_6Me_6) were generated in high yield (Scheme 1). In the FAB mass spectra the *m*/*z* value of **2b** is 918, corresponding to the molecular peak, whereas the *m*/*z* values of **2a** and **2c** are 582 and 578, respectively. These values correspond to $[M - Cl - dithiane]^+$, probably suggesting the increased stability of the iridium complex.

In the ^{1}H NMR spectrum of **2a** in $CDCl_3$, the resonances due to Cp* protons appeared at δ 1.60 and 1.67 in a *ca.* 1 : 1.1 intensity ratio at 23 °C, showing the presence of two isomers. The methylene protons appeared at δ 2.23 as a quintet due to $-CH_2-$ protons, and at δ 2.99 and 4.15 as broad resonances, being at lower magnetic fields than those in free dithiane. At −20°, the resonance at *ca.* 4.1 disappeared and other resonances became broad. The intensity ratio of Cp* resonances is *ca.* 1 : 1.5. At −40 °C, several broad resonances began to appear and a relative population is 1 : 2.0. At −60 °C, two sets of methylene groups were observed at δ 2.0–4.8, in which the SCH_2S protons showed well-resolved AB systems centered at δ 4.05 and 4.39 with coupling of $J_{HH} = 13.0$ Hz. At this temperature, both of ring reversal and sulfur inversion are slow on the NMR time scale and the relative populations of the two conformers were calculated to be 1 : 2.6. A similar behavior has been reported in the molybdenum complexes.[14] The ^{1}H NMR spectrum of **2a** in CD_3COCD_3 at room temperature indicated only a singlet at δ 1.70 for Cp* protons and that at −60 °C still remained as only one singlet, suggesting that this behavior depends on either the absence of isomers or the rapid exchange between two isomers in CD_3COCD_3. Based on ^{1}H NMR spectra in $CDCl_3$ at room temperature, the ruthenium complex

2c showed the presence of isomers consisting of *ca.* 1 : 2 molar ratio, whereas the iridium complex **2b** showed the absence of isomers.

Since the X-ray analyses of **2a** and **2b**[15] revealed that the 1,3-dithiane ligand adopted a chair-form and the Cp^*MCl_2 moieties were connected to each S atom at the equatorial positions (*vide infra*) (Fig. 1), there are two possible isomers for the complex depending on whether the two Cp^*Cl_2M moieties are equatorial or axial to the ligand ring.

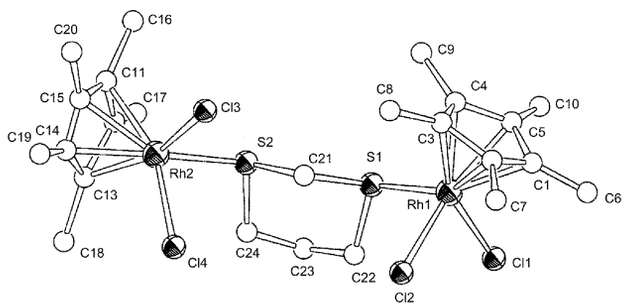

Fig. 1 Molecular structure for **2a**.

Since the isomer B bearing the metal fragments connected to the equatorial positions is more stable than the isomer A bearing metal fragments connected to the axial positions, we assigned the chemical shift of δ 1.67 to the isomer A and that of δ 1.60 to the isomer B for **2a**.

Reactions of **1a**, **1b** or **1c** with a large excess of 1,3-dithiane gave brown or orange complexes of $[(Cp^*MCl_2)(C_4H_8S_2)]$ (**3a**: M = Rh; **3b**: M = Ir) or $[\{(p\text{-cymene})RuCl_2\}(C_4H_8S_2)]$ **3c**, whereas a C_6Me_6 complex **1d** generated **2d** exclusively without formation of a mononuclear complex. It was confirmed by X-ray analyses of **3a** and **3c**[15] that the Cp^*Cl_2Rh and (*p*-cymene)Ru moieties coordinated one of the S atoms at an equatorial position (Fig. 2). In the FAB mass spectrum of **3**, the highest masses were fragments such as $[Cp^*MCl]^+$ or $[(p\text{-cymene})RuCl]^+$ without showing the molecular peaks.

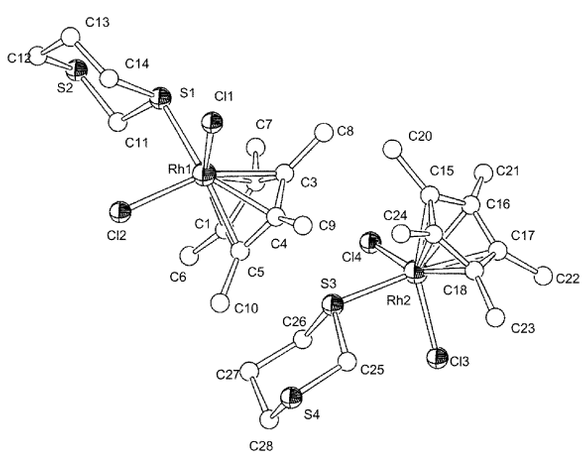

Fig. 2 Molecular structure for **3a**.

The absorption spectra of mono-nuclear complexes appeared at λ_{max} 415 nm for **3a**, at λ_{max} 335 nm for **3b**, and at λ_{max} 426 and 356 nm for **3c**, showing a pattern closely similar to the spectrum of the corresponding binuclear complex and the absorption bands blue-shifted slightly; at λ_{max} 418 nm for **2a**, at λ_{max} 340 nm for **2b**, and at λ_{max} 434 and 354 nm for **2c**.

Heteronuclear complexes

Treatment of rhodium complex **3a** with **1b** in a 2 : 1 molar ratio generated a heterometallic complex **2ab**, $[(Cp^*RhCl_2)(Cp^*IrCl_2)(\mu\text{-}1,3\text{-}S_2C_4H_8)]$. Analogously, **2ab** was generated from the reaction of **3b** with $[Cp^*RhCl_2]_2$. The ^1H NMR spectrum showed only one singlet for Cp* protons, due to an accidental degeneracy of the chemical shift. The UV-vis spectrum showed two absorption bands at λ_{max} 414 and 340 nm, in which the former band corresponds to the λ_{max} values of **2a** or **3a** and the latter to those of **2b** or **3b**.

Analogous reactions of **2a** or **2b** with the ruthenium complex **1c** gave each homonuclear complex without forming the corresponding heteronuclear complex. The reverse reactions of **3c** with **1a** or **1b** also generated each homonuclear complex. Heteronuclear complexes bearing the ruthenium moiety could not be isolated. A similar trend has been noted in the chemistry of 1,8-[bis(diphenylphosphinomethyl)]naphthalene.[16]

Ionic complexes

Ionic complexes of (arene)ruthenium(II), $[(arene)RuCl(1,3\text{-}S_2C_4H_8)_2](X)$ (arene = C_6H_6 for X = PF_6 and C_6Me_6 for X = BPh_4), bearing 1,3-dithiane have been briefly described by Stephenson and his coworkers.[17] We extended their chemistry to rhodium and iridium complexes. Reaction of **1b** with two or more equivalents of KPF_6 in the presence of an excess of 1,3-dithiane in methanol or acetone gave orange–red complex $[Cp^*IrCl(1,3\text{-}S_2C_4H_8)_2](PF_6)$ **4b**. In the FAB mass spectrum, the highest peak of *m*/*z* 603 corresponds to the molecular cation and the base peak is *m*/*z* 483, corresponds to $[Cp^*IrCl(1,3\text{-}S_2C_4H_8)]^+$. The IR spectrum showed the presence of a PF_6 anion absorption at 835 cm^{-1}. The ^1H NMR spectrum showed a singlet at δ 1.87 due to Cp* protons. Complexes of rhodium and ruthenium, $[Cp^*RhCl(1,3\text{-}S_2C_4H_8)_2](PF_6)$ **4a** and $[(p\text{-cymene})RuCl(1,3\text{-}S_2C_4H_8)_2](PF_6)$ **4c**, can be prepared in a similar way. The UV-vis. spectra of the ionic complexes are closely similar to those found for neutral mononuclear or binuclear complexes, and the λ_{max} values appeared at shorter wavelengths than those found in mono- or dinuclear complexes; at λ_{max} 397 nm for **4a**, at λ_{max} 317 nm for **4b**, and at λ_{max} 407 and 334 nm for **4c**. The λ_{max} values decreased with the number of dithiane ligand per metal ion. The detailed structure is confirmed by X-ray analysis of **4a** (Fig. 3).

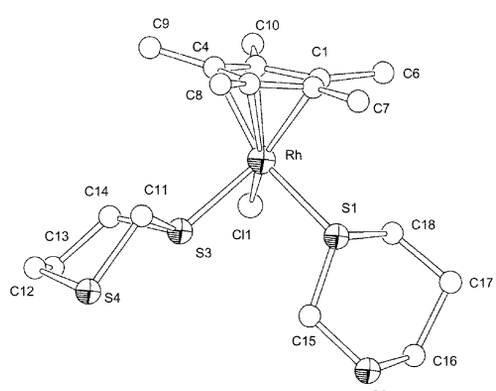

Fig. 3 Molecular structure for **4a**; the PF_6 anion was omitted for clarity.

Reactions of 4

Complexes **4** have potential for construction of complexes with high nuclearity, because they contain two uncoordinated sulfur atoms in the molecules. Complexes **4a** and **4b** were treated with **1a**, **1b** or **1c** in a 1 : 1 molar ratio, giving corresponding trinuclear complexes $[\{Cp^*Rh(1,3\text{-}S_2C_4H_8)_2\}\{(p\text{-cymene})RuCl_2\}_2](PF_6)$ **5ac**, $[\{Cp^*Ir(1,3\text{-}S_2C_4H_8)_2\}(Cp^*MCl_2)_2](PF_6)$ (**5ba**: M = Rh; **5bb**: M = Ir) or $[\{Cp^*Ir(1,3\text{-}S_2C_4H_8)_2\}\{(p\text{-cymene})RuCl_2\}_2](PF_6)$ **5bc**.

In the ^1H NMR spectra of **5ba**, Cp* protons appeared at δ 1.66 and 1.74 as singlets consisting of a 1 : 2 intensity ratio. The UV-vis spectra showed two absorption bands at λ_{max} 408 and *ca.* 340 nm; these bands are in good agreement with those found in each complex of rhodium(III) and iridium(III). The ^1H

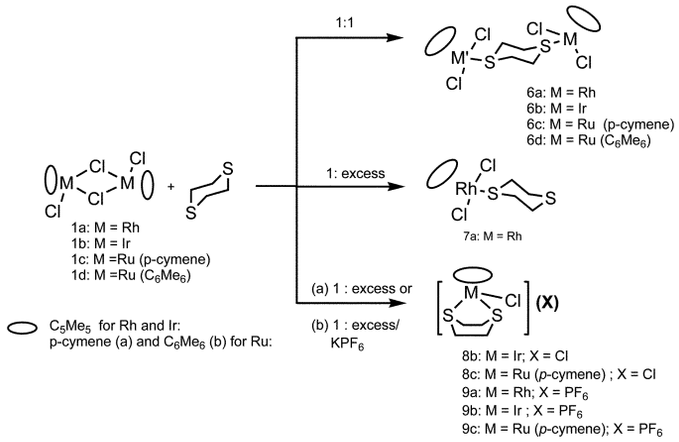

Scheme 2 Reactions of 1,4-dithiane.

NMR spectrum of **5bc** showed a doublet at δ 1.29 and a singlet at δ 1.66 with an intensity ratio of 4 : 5, due to isopropyl and Cp* protons, respectively. The UV-vis spectrum showed two absorption bands at λ_{max} 420 and 343 nm, reminiscent of the presence of ruthenium and iridium moieties. Similar spectroscopic behaviors were observed for other trinuclear complexes. In these UV-vis spectra, characteristic absorptions responsible for metal moieties were observed for all trinuclear complexes. These trinuclear complexes are the promising potentials for formation of complexes bearing more highly nuclearity.

Preparation of complexes bearing 1,4-dithiane

Complexes **1a**, **1c** or **1d** were treated with 1,4-dithiane in a 1 : 1 molar ratio, giving [{Cp*MCl_2}$_2$(1,4-$S_2C_4H_8$)] (**6a**: M = Rh; **6b**: M = Ir) or [{(arene)$RuCl_2$}$_2$(1,4-$S_2C_4H_8$)] (**6c**: arene = *p*-cymene; **6d**: arene = C_6Me_6) (Scheme 2).

The UV-vis spectra showed an absorption band at λ_{max} 420 nm for **6a** and two bands for ruthenium complexes appeared at λ_{max} 420 and 351 nm for **6c**, and at λ_{max} 449 and 350 nm for **6d**. These spectral patterns are similar to those found in 1,3-dithiane complexes. The ^{1}H NMR spectra of these complexes showed the presence of isomers. Two resonances for Cp* protons of **6a** appeared at δ 1.60 and 1.66 consisting of a 1.2 : 1.0 intensity ratio. A similar behavior was observed in **6d**, consisting of a 1.1 : 1.0 intensity ratio. There are two possible isomers for the complex depending on whether the two Cp*Cl_2M moieties are equatorial or axial to the ligand ring. Since the relative populations of the two conformers are smaller than those found for 1,3-dithiane complexes, the barrier between two conformers is probably very small. This is the result of releasing steric repulsive interaction between two metal moieties in the 1- and 4-positions. Probably, the structure with each Ru moiety in the equatorial positions of the ligand ring is more stable than that in the axial positions. In some attempts to prepare mono-nuclear complexes, the reaction with a large amount of 1,4-dithiane was carried out, generating Cp*MCl_2(1,4-$S_2C_4H_8$) (**7a**: M = Rh; **8b**: M = Ir) or (*p*-cymene)$RuCl_2$(1,4-$S_2C_4H_8$) **8c**, respectively. The UV-vis spectra showed λ_{max} 333 nm for **8b** and λ_{max} 401 and 329 nm for **8c**. The ^{1}H NMR spectrum of **7a** showed three singlets at δ 1.59, 2.82 and 3.31, consisting of an intensity ratio of 15 : 4 : 4, whereas those of **8b** and **8c** showed four doublets which each corresponds to two methylene protons; at δ 3.06, 3.24, 3.49 and 3.97 for the former and at δ 2.86, 3.15, 3.56 and 3.83 for the latter. The spectrometric data of **7a** suggested a structure with a S atom of the 1,4-dithiane ligand coordinated to the Rh atom. However, two other complexes **8b** and **8c** do not correspond to the structure of **7a**. The structures are considered to be mononuclear ionic complexes in which 1,4-dithiane acts as a chelating ligand. In fact X-ray analysis of **8b** was in agreement with the proposed structure (Fig. 4).

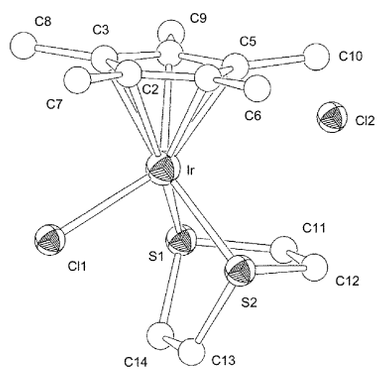

Fig. 4 Molecular structure for **8b**.

Complexes **1a**, **1b** and **1c** were treated with an excess of 1,4-dithiane in the presence of KPF_6, generating [Cp*MCl(1,4-$S_2C_4H_8$)](PF_6) (**9a**: M = Rh; **9b**: M = Ir) or [(*p*-cymene)RuCl(1,4-$S_2C_4H_8$)](PF_6) **9c**, respectively. The molecular peaks of **9a** and **9b** in the FAB mass spectrum are *m*/*z* 394 and 483, respectively, being the values of the corresponding cations. It was confirmed by X-ray analysis of **9c** that the molecule has a chelate structure consisting of a boat form, suggesting high stability of a five-membered ring (Fig. 5). This structure is similar to that of **8b** and **8c**.

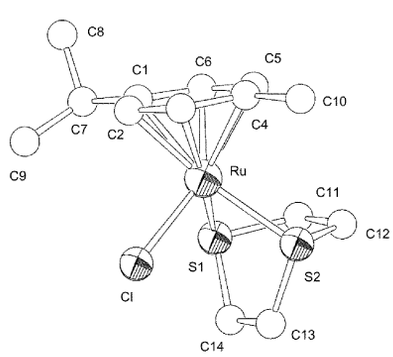

Fig. 5 Molecular structure for **9c**; the PF_6 anion was omitted for clarity.

The ^{1}H NMR spectrum of **9c** showed two doublets at δ 5.61 and 5.84 for methylene protons. This spectrum is in disagreement with the structure in the solid state, probably resulting in occurrence of the fast exchange of the ligand. However, methylene protons appeared as four doublets at δ 2.79, 2.99, 3.22 and 3.34 for **9a**, and at δ 2.74, 2.82, 3.21 and 3.39 for **9b**, respectively, corresponding to the structure in the solid state. The UV-vis spectrum showed a strong absorption band for **9a** and **9b**, and two strong bands for **9c**: at λ_{max} 393 nm for **9a**, at λ_{max} 335 nm for **9b** and at λ_{max} 401 and 325 nm for **9c**. Discordances of ^{1}H

Table 2 Selected bond lengths (Å) and angles (°) for [{Cp*$RhCl_2$}$_2$(1,3-$S_2C_4H_8$)]2CH_2Cl_2 **2a**

Rh(1)–Cl(1)	2.411(2)	Rh(1)–Cl(2)	2.395(2)	Rh(1)–S(1)	2.377(2)
Rh(2)–Cl(3)	2.426(2)	Rh(2)–Cl(4)	2.415(4)	Rh(2)–S(2)	2.374(2)
Cl(1)–Rh(1)–Cl(2)	90.57(8)	Cl(1)–Rh(1)–S(1)	86.18(8)	Cl(2)–Rh(1)–S(1)	91.26(8)
Cl(3)–Rh(2)–Cl(4)	93.45(9)	Cl(3)–Rh(2)–S(3)	86.78(7)	Cl(4)–Rh(2)–S(2)	89.99(8)
Rh(1)–S(1)–C(21)	98.6(4)	Rh–S(1)–C(22)	102.1(4)	C(21)–S(1)–C(22)	97.4(6)
Rh(2)–S(2)–C(21)	99.5(4)	Rh(2)–S(2)–C(24)	102.9(4)	C(21)–S(2)–C(24)	96.3(6)

Table 3 Selected bond lengths (Å) and angles (°) for [Cp*$RhCl_2$(1,3-$S_2C_4H_8$)] **3a**

Rh(1)–Cl(1)	2.428(2)	Rh(1)–Cl(2)	2.402(3)	Rh(1)–S(1)	2.386(3)
Rh(2)–Cl(3)	2.423(3)	Rh(2)–Cl(4)	2.413(3)	Rh(2)–S(3)	2.389(3)
Cl(1)–Rh(1)–Cl(2)	94.9(1)	Cl(1)–Rh(1)–S(1)	85.39(9)	Cl(2)–Rh(1)–S(1)	89.9(1)
Cl(3)–Rh(2)–Cl(4)	93.7(1)	Cl(3)–Rh(2)–S(3)	90.4(1)	Cl(4)–Rh(2)–S(3)	87.1(1)
Rh(1)–S(1)–C(11)	106.5(4)	Rh(1)–S(1)–C(14)	107.1(4)	C(11)–S(1)–C(14)	100.6(5)
Rh(2)–S(3)–C(25)	105.0(4)	Rh(2)–S(3)–C(26)	107.9(4)	C(11)–S(2)–C(12)	101.0(6)

Table 4 Selected bond lengths (Å) and angles (°) for [Cp*RhCl(1,3-$S_2C_4H_8$)$_2$](PF_6)·CH_2Cl_2 **4a**

Rh(1)–Cl(1)	2.393(8)	Rh(1)–S(1)	2.395(8)	Rh(1)–S(3)	2.39(1)
Cl(1)–Rh(1)–S(1)	92.1(4)	Cl(1)–Rh(1)–S(3)	81.6(5)	S(1)–Rh(1)–S(3)	89.8(3)
Rh(1)–S(1)–C(15)	115(1)	Rh(1)–S(1)–C(18)	101(1)	C(15)–S(1)–C(18)	102(1)
Rh(1)–S(3)–C(11)	114(2)	Rh(2)–S(3)–C(14)	113(1)	C(15)–S(2)–C(16)	101(2)
C(11)–S(4)–C(12)	93(2)				

Table 5 Selected bond lengths (Å) and angles (°) for [Cp*IrCl(μ-1,4-$S_2C_4H_8$)]Cl **8b**

Ir(1)–Cl(1)	2.404(2)	Ir(1)–S(1)	2.348(2)	Ir(1)–S(2)	2.358(3)
Cl(1)–Ir(1)–S(1)	90.21(9)	Cl(1)–Ir(1)–S(2)	90.95(9)	S(1)–Ir(1)–S(2)	76.24(9)
Ir(1)–S(1)–C(11)	100.2(3)	Ir(1)–S(1)–C(14)	102.7(4)	C(11)–S(1)–C(14)	96.6(5)
Ir–S(2)–C(12)	100.7(4)	Ir–S(2)–C(13)	102.1(3)	C(12)–S(2)–C(13)	95.6(5)

Table 6 Selected bond lengths (Å) and angles (°) for [(*p*-cymene)RuCl(μ-1,4-$S_2C_4H_8$)](PF_6) **9c**

Ru–Cl	2.398(3)	Ru–S(1)	2.368(3)	Ru–S(2)	2.384(3)
Cl–Ru–S(1)	89.1(1)	Cl–Ru–S(3)	87.0(3)	S(1)–Ru–S(2)	75.6(1)
Ru–S(1)–C(11)	98.6(4)	Ru–S(1)–C(14)	102.1(4)	C(11)–S(1)–C(14)	97.4(6)
Ru–S(2)–C(12)	99.5(4)	Ru–S(2)–C(13)	102.9(4)	C(12)–S(2)–C(13)	96.3(6)

NMR spectra between **8b** and **9b**, and **8c** and **9c**, in which each cationic species is similar, are the results of different anions, suggesting interaction between anionic and cationic species in solutions. Neutral and ionic complexes **7a** and **8** reacted readily with **1**, generating the corresponding binuclear complexes.

Molecular structures

Crystal structures of 2a and 3a. Perspective drawings of **2a** and **3a** with the atomic numbering scheme are given in Figs. 1 and 2 and selected bond lengths and angles are listed in Tables 2 and 3. The 1,3-$S_2C_4H_8$ ligand adopts a chair form and two Cp*$RhCl_2$ moieties occupy the equatorial positions of the ring ligand. The average Rh–Cl bond length (2.412 Å) for **2a** is not significantly different from that (2.419 Å) for **3a**. The average Rh–S bond length of 2.376 Å for **2a** is somewhat shorter than that (2.388 Å) for **3a**. The average Cl–Rh–Cl bond angles are 92.0° for **2a** and 94.3° for **3a**, respectively, being wider than the average Cl–Rh–S angle of 88.3° for both complexes.

Crystal structure of 2ab. The crystals decayed finally by 85%. Since the accuracy is too low to discuss the bond lengths and angles, they are omitted.[15] The metal atoms have occupancies of 0.5 for Ir and Rh atoms. The 1,3-$S_2C_4H_8$ ligand adopts a chair-form as in other complexes. The metal fragments occupy the equatorial positions.

Crystal structure of 4a. A perspective drawing of **4a** with the atomic numbering scheme is given in Fig. 3 and selected bond lengths and angles are listed in Table 4. The molecule is an ionic complex, and the rhodium atom is surrounded by a Cp*, two 1,3-dithiane ligands, and a Cl atom. The two 1,3-dithiane ligands adopt the chair forms. The Cp*ClRh moiety is located in an equatorial position. The Rh(1)–Cl(1) length of 2.393(8) Å is somewhat shorter than those in the range 2.395–2.431 Å found for neutral Rh complexes, but the average Rh–S length of 2.392 Å is compared with those in the range 2.374–2.395 Å for the neutral ones.

Crystal structures of 8b and 9c. The perspective drawings with the atomic numbering scheme are given in Figs. 4 and 5, and selected bond lengths and angles are listed in Tables 5 and 6. The molecules have the ionic structures: the anions are a Cl ion for **8b** and a PF_6 ion for **9c**, and the cationic molecules each consist of two five-membered rings with the 1,4-dithiane acting as a bidentate ligand. It adopts a boat form. The Ir–Cl(1) length of 2.404(2) Å and Ru–Cl bond of 2.398(3) are not significantly different from those (2.403(4) Å for **2b** and 2.398(4) Å for **3c**) found in the corresponding neutral complexes. The average Ir–S bond of 2.353 Å is similar to that (2.356(4) Å) for the neutral complex **2b**, but is somewhat shorter than those found in neutral and ionic rhodium complexes **2a**, **3a** and **4a**. The S(1)–M–S(2) bite angles of 76° are narrower than the S(1)–Rh(1)–S(3) angle of 90° for **4a**, resulting in the chelating ligand.

Conclusion

We have expected formation of polymetallic complexes bearing 1,4-dithiane ligands, but the reactions led to formation of chelate complexes, because of high stability of five-membered ring. The 1,3-dithiane ligand was found to be superior to the 1,4-dithiane ligand for syntheses of polymetallic complexes and is expected to serve as a precursor of high nuclear complexes.

Acknowledgements

We thank Professor Shigetoshi Takahashi and Dr. Fumie Takei for The Institute of Scientific and Industrial Research, Osaka University for measurements of FAB mass spectroscopy. This work was partially supported by the Grant-in-Aid for Scientific Research from the Ministry of Education, Science, Culture, and Sports, Japan.

References and notes

1 "*Supramolecular Architecture*": (*a*) R. Robson, B. F. Abraham, S. R. Batten, R. W. Gable, B. F. Hoskins and J. Liu, *ACS Symp. Ser*, 1992, **499**, 256; (*b*) *Comprehensive Supramolecular Chemistry*, ed. J.-M Lehn, J. L. Atwood, J. E. D. Davies, D. D. MacNicol and F. Vogtle, Pergamon Press, Oxford, 1995, vol. 1–11; (*c*) P. L. Stang and B. Oleyuk, *Acc. Chem. Res.*, 1997, **30**, 502; (*d*) M. Fujita and K. Ogura, *Coord. Chem. Rev.*, 1996, **148**, 249; (*e*) B. Olenyuk, A. Fechtenkotter and P. J. Stang, *J. Chem. Soc., Dalton Trans.*, 1998, 1707 and references therein.

2 (*a*) A. Mayr and J. Guo, *Inorg. Chem.*, 1999, **38**, 921; (*b*) J. A. Whiteforld, P. J. Stang and S. D. Huang, *Inorg. Chem.*, 1998, **37**, 5795; (*c*) J. Manna, C. J. Kuehl, J. A. Whiteford, P. J. Stang, D. C. Muddiman, S. A. Hofstadler and R. D. Smith, *J. Am. Chem. Soc.*, 1997, **119**, 11611 and references therein; (*d*) P. J. Stang, J. Fan and B. Olenyuk, *Chem. Commun.*, 1997, 1453; (*e*) J. A. Whitefold, C. V. Lu and P. J. Stang, *J. Am. Chem. Soc.*, 1997, **119**, 2524 and references therein; (*f*) S.-S. Sun and A. J. Lees, *J. Am. Chem. Soc*, 2000, **122**, 8956; (*g*) S. Leninoger, B. Olenyuk and P. J. Stang, *Chem. Rev.*, 2000, **100**, 853; (*h*) N. Takeda, K. Umemoto, K. Yamaguchi and M. Fujita, *Nature*, 1999, **398**, 794.

3 (*a*) H. Suzuki, N. Tajima, K. Tatsumi and Y. Yamamoto, *Chem. Commun.*, 2000, 1801; (*b*) Y. Yamamoto, H. Suzuki, N. Tajima and K. Tatsumi, *Chem. Eur. J.*, 2002, **8**, 372–379.

4 (*a*) M. Schroder, *Pure Appl. Chem.*, 1988, **60**, 517; (*b*) A. J. Blake and M. Schroder, *Adv. Inorg. Chem.*, 1990, 2; (*c*) S. R. Cooper, *Acc. Chem. Res.*, 1988, **21**, 141.

5 (*a*) R. S. Ashworth, C. K. Prout, A. Domenicano and A. Vaciago, *J. Chem. Soc. A*, 1968, 93; (*b*) W. R. Costello, A. T. McPhail and G. A. Sim, *J. Chem. Soc. A*, 1966, 1190; (*c*) T. Bjorvatten, *Acta Chem. Scand.*, 1966, **20**, 1863; (*d*) G. Kiel and R. Engler, *Chem. Ber.*, 1974, **107**, 3444; (*e*) M. Schmidt, R. Bender, J. Ellermann and H. Gbelein, *Z. Anorg. Allg. Chem.*, 1977, **437**, 155; (*f*) J. D. Donaldson and D. G. Nicholson, *J. Chem. Soc. A*, 1970, 145; (*g*) J. S. Filippo, H. J. Sniadoch and R. L. Grayson, *Inorg. Chem.*, 1974, **13**, 2121; (*h*) S. R. Wade and G. R. Willey, *Inorg. Chim. Acta*, 1983, **72**, 201–204.

6 (*a*) E. W. Abel, M. Booth and K. G. Orrell, *J. Chem. Soc., Dalton Trans.*, 1980, 1582; E. W. Abel, A. R. Khan, K. Kite and K. G. Orrell, *J. Chem. Soc., Dalton Trans.*, 1977, 194 and references therein; (*b*) E. W. Abel, M. Booth, K. G. Orrell and G. M. Pring, *J. Chem. Soc., Dalton Trans.*, 1981, 1944.

7 C. White, A. Yates and P. M. Maitlis, *Inorg. Synth.*, 1992, **29**, 228.

8 J. W. Kang, K. Moseley and P. M. Maitlis, *J. Organomet. Chem.*, 1975, **87**, 359.

9 (*a*) M. A. Bennett and A. K. Smith, *J. Chem. Soc., Dalton Trans.*, 1974, 233; (*b*) M. A. Bennett, T.-N. Hung, T. W. Matheson and A. K. Smith, *Inorg. Synth.*, 1982, **21**, 74; (*c*) M. A. Bennett, T. W. Matheson, G. B. Robertson, A. K. Smith and P. A. Tucker, *Inorg. Chem.*, 1980, **19**, 1014.

10 D. T. Cromer and J. T. Waber, *International Tables for X-ray Crystallography*, Kynoch Press, Birmingham, UK, 1974, Table 2.2A.

11 J. A. Ibers and W. C. Hamilton, *Acta Crystallogr.*, 1964, **17**, 718.

12 D. C. Creagh and W. J. McAulley, *International Tables for Crystallography*, Kluwer, Boston, 1992, Vol. C, Table 4.2.6.8, pp. 219–222.

13 TEXSAN: Crystal Structure Analysis Package, Molecular Structure Corporation Houston, TX, 1985 and 1992.

14 E. W. Abel, M. Booth, K. G. Orrell and G. M. Pring, *J. Chem. Soc., Dalton Trans.*, 1981, 1944.

15 The crystal data and molecular structure are given as ESI †.

16 Y. Yamamoto and F. Miyauchi, *Inorg. Chim. Acta*, 2002, **334**, 77; Y. Yamamoto and F. Miyauchi, *Inorg. Chim. Acta*, 2002, **334**, 1571.

17 D. A. Tocher, R. O. Gould, T. A. Stephenson, M. A. Bennett, J. P. Ennett, T. W. Matheson and L. S. V. K. Shah, *J. Chem. Soc., Dalton Trans.*, 1983, 1571.